
Stackelberg Game Preference Optimization for Data-Efficient Alignment of Language Models

Xu Chu^{1,2} Zhixin Zhang³ Tianyu Jia^{4,2} Yujie Jin^{4,2}

Abstract

Aligning language models with human preferences is critical for real-world deployment, but existing methods often require large amounts of high-quality human annotations. Aiming at a data-efficient alignment method, we propose *Stackelberg Game Preference Optimization (SGPO)*, a framework that models alignment as a two-player Stackelberg game, where a policy (leader) optimizes against a worst-case preference distribution (follower) within an ϵ -Wasserstein ball, ensuring robustness to (self-)annotation noise and distribution shifts. SGPO guarantees $\mathcal{O}(\epsilon)$ -bounded regret, unlike Direct Preference Optimization (DPO), which suffers from linear regret growth in the distribution mismatch. We instantiate SGPO with the *Stackelberg Self-Annotated Preference Optimization (SSAPO)* algorithm, which iteratively self-annotates preferences and adversarially reweights synthetic annotated preferences. Using only 2K seed preferences, from the UltraFeedback dataset, i.e., 1/30 of human labels in the dataset, our method achieves 35.82% GPT-4 win-rate with Mistral-7B and 40.12% with Llama3-8B-Instruct within three rounds of SSAPO.

1. Introduction

Recent breakthroughs in large language models (LLMs) have made it increasingly crucial to *align* generated text with human preferences for both usability and safety (Ouyang et al., 2022; Bai et al., 2022). Traditional approaches such as Reinforcement Learning from Human Feedback (RLHF) (Christiano et al., 2017) and Direct Preference Optimization (DPO) (Rafailov et al., 2023) often require *massive* amounts of meticulously curated preference data. Not only is gathering such a dataset expensive and time-consuming, but any mislabeling can propagate through iterative alignment stages (Casper et al., 2023), leading to suboptimal or even unsafe model behaviors. This raises a critical challenge: *How can we achieve preference data-efficient alignment of language models while maintaining robustness to annotation noise?*

From the perspective of data efficiency and robustness, existing alignment approaches often suffer from two main issues: *Self-annotation gaps* and *Lack of equilibrium guarantees under noise*. Recent work explores self-annotation (Lee et al., 2024; Yuan et al., 2024; Kim et al., 2025), where an LLM generates labels for new prompt-response pairs instead of relying on humans. While this indeed lowers annotation cost, such methods often treat policy updates and preference annotation as disconnected processes. Consequently, once noisy synthetic preferences are generated, there is limited recourse if the LLM’s self-labels embed systematic biases or errors that can corrupt future training (Chowdhury et al., 2024). Some adversarial training approaches (Cheng et al., 2023; Wu et al., 2024a) attempt to counter distributional shifts in preference data, but they often lack formal *equilibrium* guarantees and can lead to unstable optimization cycles in practice. Furthermore, these adversarial approaches are not specifically tailored for data-scarce alignment regimes, thus limiting their applicability when human labels are extremely expensive. *We delay a more thorough related work section in the Appendix A.*

To address these issues, we propose **Stackelberg Game Preference Optimization (SGPO)**, a framework that models alignment as a *two-player* Stackelberg game between: a *policy* (the leader), which aims to satisfy real human preferences, and an *adversarial preference distribution* (the follower), which explores worst-case shifts within a defined Wasserstein ball of radius ϵ . Drawing inspiration from Stackelberg dynamics (Başar & Olsder, 1998) and optimal transport (Villani et al., 2009), SGPO ensures that the policy optimizes against the worst plausible shifts in preference data. Specifically, under ϵ -bounded shifts (or annotation noise), we prove that the resulting policy’s regret is at most $\mathcal{O}(\epsilon)$ (see Section 2), whereas standard DPO can incur *linear* regret growth with respect to the magnitude of distribution mismatch. Although our analysis uses ϵ -Wasserstein balls as a tractable model of moderate noise or mismatch, it remains relevant for practical alignment scenarios where annotation errors are not unbounded but still matter.

On top of SGPO, we develop the **Stackelberg Self-Annotated Preference Optimization (SSAPO)** (Section 3) algorithm, a procedure aimed at drastically lowering human annotation needs. SSAPO starts with a small human-labeled seed (about 1/30 of the usual scale in our experiments) and then: (1) *Self-Annotates* newly sampled prompts by generating responses and extracting winner–loser pairs from the current policy’s own comparisons. (2) *Adversarially Reweights* these pairs within a Wasserstein ball of radius ϵ , by solving a distributionally robust optimization (DRO) (Mohajerin Esfahani & Kuhn, 2018) program, ensuring that potentially corrupted or unrepresentative synthetic preferences do not overwhelm the policy update. By iterating these two steps, SSAPO instantiates the SGPO framework, preserving theoretical bounded-regret guarantees while yielding significant data-efficiency gains. In practice, we find that with only 1/30 of the usual human annotations (from the UltraFeedback dataset (Cui et al., 2023)), SSAPO attains 35.82 % GPT4 win-rate (24.44% LC win-rate) on Mistral-7B, 40.12% win-rate (33.33% LC win-rate) on Llama3-8B-instruct. Which matches Mixtral Large (21.4% win-rate and 32.7% LC win-rate) and Llama3-70B-instruct (33.2% winrate and 34.4% LC win-rate) according to the AlphacaEval 2.0 leaderboard (Dubois et al., 2024b).

In summary, We formulate DPO-like alignment as a Stackelberg game, demonstrate *existence* of an equilibrium, and establish that *SGPO* achieves an $\mathcal{O}(\epsilon)$ regret bound under ϵ -bounded noise, in contrast to the linear regret behavior of DPO when facing similarly scaled shifts.(Section 2). We implement SGPO via *SSAPO*, which combines self-annotation with distributionaly robust optimization.(Section 3) Extensive experiments show that SSAPO attains strong alignment performance with substantially fewer human labels, thereby showing its real-world viability for cost-effective preference alignment of LLMs (Section 4).

2. Theoretical Foundation: Stackelberg Game Preference Optimization Framework

In this section, we introduce our *Stackelberg Game Preference Optimization* (SGPO) framework. First, we recap the standard DPO approach (Section 2.1). We then formulate SGPO as a two-player Stackelberg game (Section 2.2), prove the existence of an equilibrium and characterize its convergence under iterative updates (Sections 2.3). Lastly, we provide a regret analysis (Section 2.4), showing that SGPO suffers at most $\mathcal{O}(\epsilon)$ regret under ϵ -bounded shifts, while DPO’s regret can grow linearly in the distribution mismatch. Proofs in this section is delayed to Appendix D.

2.1. Preliminaries: Preference Datasets and DPO

Preference-Ranked Dataset. We consider a dataset $D = \{(x^i, y_w^i, y_l^i)\}_{i=1}^N$, where x^i is a prompt (or context), and (y_w^i, y_l^i) denote the *winner* and *loser* responses. This dataset is generally obtained by human judgments or, in some cases, by partial self-annotation.

RLHF and KL Regularization. Classical RL from Human Feedback (RLHF; (Christiano et al., 2017)) trains a parameterized policy π_θ by maximizing a reward $R(x, y)$ subject to staying close to a reference policy π_{ref} . A common formulation is:

$$\max_{\theta \in \Theta} \mathbb{E}_{x \sim \mathcal{D}, y \sim \pi_\theta(\cdot | x)} \left[R(x, y) - \beta D_{\text{KL}}(\pi_\theta(\cdot | x) \| \pi_{\text{ref}}(\cdot | x)) \right], \quad (1)$$

where β controls the strength of the KL penalty. The distribution \mathcal{D} is typically the distribution of prompts seen during training or evaluation.

Direct Preference Optimization (DPO). Rafailov et al. (2023) introduced an alternative that bypasses explicit reward modeling (i.e., estimating $R(x, y)$ seperately) by leveraging the Bradley-Terry (BT) pairwise preference model:

$$p(y_w \succ y_l | x) = \sigma(R(x, y_w) - R(x, y_l)),$$

where $\sigma(z) = \frac{1}{1+e^{-z}}$. Under first-order optimality of a related KL-regularized objective, the optimal reward for a given policy π_θ must take the form

$$R(x, y) = \beta \log \frac{\pi_\theta(y | x)}{\pi_{\text{ref}}(y | x)} + \beta \log Z(x), \quad (2)$$

with $Z(\cdot)$ a partition function. Substituting this form into the BT model yields a *direct* method to optimize θ by maximum likelihood optimization with preference pairs,

$$\mathcal{L}_{\text{DPO}}(\theta) = \max_{\theta \in \Theta} \mathbb{E}_{-\log(x, y_w, y_l) \sim D} \left[\log \sigma(R(x, y_w) - R(x, y_l)) \right]. \quad (3)$$

Despite its appealing simplicity, DPO lacks a built-in mechanism for handling shifts away from the empirical distribution of preferences in D . As a result, if future or adversarial data differ substantially from the training set, DPO can incur large performance drops (Chowdhury et al., 2024). This motivates a more robust approach.

2.2. SGPO: A Two-Player Stackelberg Game

We propose to defend against distributional uncertainty by treating the learning process as a two-player Stackelberg game (Başar & Olsder, 1998). Concretely:

- **Policy (the leader):** A policy model π_θ , parameterized by $\theta \in \Theta \subset \mathbb{R}^d$. This player chooses a parameter θ to *maximize* its worst-case expected performance (likelihood) against an adversarial preference distribution.
- **Adversarial Preference Distribution (the follower):** A distribution P over pairwise outcomes (y_w, y_l) . This player chooses, *after* seeing θ , a preference distribution within an ϵ -ball of the empirical distribution \hat{P} ¹. The follower's goal is to *minimize* the policy's performance.

To formalize “ ϵ -ball,” we adopt the 1-Wasserstein distance (Cf. Appendix B for more preliminaries on the Wasserstein metric space)(Villani et al., 2009) and define:

$$\mathcal{U}_\epsilon(\hat{P}) = \left\{ P \in \mathcal{P}(\mathcal{Y} \times \mathcal{Y}) \mid W(P, \hat{P}) \leq \epsilon \right\}.$$

Hence, the leader's robust objective is:

$$\max_{\pi \in \Pi} \min_{P \in \mathcal{U}_\epsilon(\hat{P})} \mathbb{E}_{(y_w, y_l) \sim P} \left[\log \sigma(R_\pi(y_w) - R_\pi(y_l)) \right], \quad (4)$$

where $R_\pi(y)$ ² is the policy-induced *logit* (akin to the reward term Eq. (2)) or more generally a function measuring how favorable y is under π . This induces the Stackelberg equilibrium:

Definition 2.1 (Stackelberg Equilibrium). A pair (π^*, P^*) is a *Stackelberg equilibrium* if

$$\pi^* \in \arg \max_{\pi \in \Pi} \min_{P \in \mathcal{U}_\epsilon(\hat{P})} \mathbb{E}_P [J(\pi, P)], \{leader\} \quad (5)$$

$$P^* \in \arg \min_{P \in \mathcal{U}_\epsilon(\hat{P})} \mathbb{E}_P [J(\pi^*, P)], \{follower\} \quad (6)$$

where

$$J(\pi, P) := \mathbb{E}_{(y_w, y_l) \sim P} \left[\log \sigma(R_\pi(y_w) - R_\pi(y_l)) \right]. \quad (7)$$

Under real-world annotation noise or the noisy self-annotation scenario considered in this paper, the “true” preference distribution can *deviate* from the empirical training data. SGPO prepares for the worst-case shift within radius ϵ . By adopting a Stackelberg perspective, we derive a policy that is simultaneously (i) high-performing on the empirical data and (ii) robust to preference shifts.

2.3. Existence and Convergence of a Stackelberg Equilibrium

Under standard regularity conditions (continuity, convexity, and compactness Villani et al. (2009); Mohajerin Esfahani & Kuhn (2018), confer Assumption C.1 for details) for distributionally robust optimization, we can prove that an Stackelberg equilibrium exist, and a natural alternating procedure converges to the Stackelberg equilibrium.

Theorem 2.2 (Existence of Stackelberg Equilibrium). *Under the regularity assumptions (Assumption C.1), the two-player game defined by*

$$\max_{\pi \in \Pi} \min_{P \in \mathcal{U}_\epsilon(\hat{P})} J(\pi, P),$$

$$\text{where } J(\pi, P) = \mathbb{E}_P \left[\log \sigma(R_\pi(y_w) - R_\pi(y_l)) \right]$$

admits at least one Stackelberg equilibrium (π^, P^*) .*

¹Throughout the paper, let $\hat{\xi}_i = R_\theta(x, y_w^i) - R_\theta(x, y_l^i), i = 1, \dots, N$, N denotes the preference sample size. Define the empirical measure $\hat{P}_N = \frac{1}{N} \sum_i \delta_{\hat{\xi}_i}$. Thus the ϵ -ball can be viewed as the neighbourhood of the observed preference distribution.

²We drop the term x in $R(x, y)$ for simplicity hereafter.

A natural alternating procedure—iteratively updating the policy to best respond against the adversary, and then updating the adversary’s distribution within the ϵ -ball—converges to the Stackelberg equilibrium. One such procedure is:

$$\begin{cases} \pi_{t+1} = \arg \max_{\pi \in \Pi} \min_{P \in \mathcal{U}_\epsilon(P_t)} J(\pi, P), \{leader\} \end{cases} \quad (8)$$

$$\begin{cases} P_{t+1} = \arg \min_{P \in \mathcal{U}_\epsilon(P_t)} J(\pi_{t+1}, P), \{follower\} \end{cases} \quad (9)$$

starting from an initial pair (π_0, P_0) . Here, we shift the center of the Wasserstein ball in each iteration to P_t .

Theorem 2.3 (Linear Convergence to Stackelberg Equilibrium). *Under the regularity assumptions (Assumption C.1), the sequence $\{(\pi_t, P_t)\}_{t \geq 0}$ generated by (8)–(9) converges to the Stackelberg equilibrium (π^*, P^*) . Moreover, the convergence is linear, i.e. there exists $\gamma < 1$ such that*

$$\rho((\pi_{t+1}, P_{t+1}), (\pi^*, P^*)) \leq \gamma \rho((\pi_t, P_t), (\pi^*, P^*)),$$

where ρ is a suitable metric (e.g., $\rho((\pi, P), (\pi', P')) = \|\pi - \pi'\| + W(P, P')$).

In practice, one may not directly implement (8)–(9), but the Theorem 2.3 shows that any procedure that approximates these alternating best-response updates can converge to the robust equilibrium. This provides a theoretical grounding for the SSAPO algorithm (to be introduced in the section 3), which combines standard gradient-based optimization with distributionally robust optimization.

2.4. Regret Analysis and Comparison with DPO

We now quantify SGPO’s performance under worst-case preference shifts. We show that SGPO enjoys an $\mathcal{O}(\epsilon)$ bound on its regret, whereas DPO can incur regret $\propto \delta$, where δ is the magnitude of distribution shift.

2.4.1. SGPO’s BOUNDED REGRET

Let π^* be the SGPO policy obtained from the robust problem (4). For any distribution $P \in \mathcal{U}_\epsilon(\hat{P})$, we define the (absolute) performance as

$$\mathcal{P}(\pi, P) = \mathbb{E}_{(y_w, y_l) \sim P} \left[\log \sigma(R_\pi(y_w) - R_\pi(y_l)) \right]. \quad (10)$$

We prove that π^* maintains high performance on *all* distributions P within ϵ -Wasserstein distance of \hat{P} . In particular, the drop from \hat{P} to any P is at most $\mathcal{O}(\epsilon)$.

Theorem 2.4 (Worst-Case Performance Guarantee for SGPO). *Under Assumption C.1, let π^* be the SGPO solution. Then for every $P \in \mathcal{U}_\epsilon(\hat{P})$,*

$$\mathcal{P}(\pi^*, P) \geq \mathcal{P}(\pi^*, \hat{P}) - L_R \epsilon. \quad (11)$$

In other words, the performance drop from \hat{P} to any $P \in \mathcal{U}_\epsilon(\hat{P})$ is at most $L_R \epsilon$.

Regret Notation. We define the regret of a policy π on a distribution P as

$$\text{Regret}(\pi, P) = \max_{\tilde{\pi}} \mathcal{P}(\tilde{\pi}, P) - \mathcal{P}(\pi, P). \quad (12)$$

If $\pi_P^* = \arg \max_{\tilde{\pi}} \mathcal{P}(\tilde{\pi}, P)$, then $\text{Regret}(\pi, P) = \mathcal{P}(\pi_P^*, P) - \mathcal{P}(\pi, P)$.

Theorem 2.5 (SGPO Regret Bound). *For the SGPO policy π^* , we have*

$$\sup_{P \in \mathcal{U}_\epsilon(\hat{P})} \text{Regret}(\pi^*, P) \leq 2 L_R \epsilon. \quad (13)$$

Thus, SGPO is robust: under any shift of at most ϵ , its regret is bounded by a constant factor of ϵ .

2.4.2. COMPARISON: DPO’S LINEAR REGRET

Recall that DPO π_{DPO} (Rafailov et al., 2023) maximizes $\mathcal{P}(\pi, \hat{P})$ (Eq. (3) with no regard for shifts away from \hat{P}). Let $\delta = W(\hat{P}, P^*)$. We show DPO can be arbitrarily suboptimal under large δ , scaling linearly with δ .

Theorem 2.6 (DPO Regret Lower Bound). *Let $\pi_{\text{DPO}} = \arg \max_{\pi} \mathcal{P}(\pi, \hat{P})$, and let P^* be a distribution satisfying $W(\hat{P}, P^*) = \delta$. Then*

$$\text{Regret}(\pi_{\text{DPO}}, P^*) \geq L_R (\delta - 2\epsilon). \quad (14)$$

In particular, if $\delta \gg \epsilon$, DPO’s regret grows linearly in δ .

Corollary 2.7 (SGPO Advantage Over DPO). *If $W(\hat{P}, P^*) = \delta > 2\epsilon$, then*

$$\frac{\text{Regret}(\pi_{\text{DPO}}, P^*)}{\text{Regret}(\pi^*, P^*)} \geq \frac{\delta - 2\epsilon}{2\epsilon}. \quad (15)$$

Thus, SGPO’s robust policy can outperform DPO by a factor of $\frac{\delta}{2\epsilon} - 1$ under sufficiently large distribution shift δ .

Discussion of Theoretical Results. Collectively, these results clarify *why* SGPO is well-suited for preference alignment: if the “true” preference distribution lies within an ϵ -Wasserstein ball of the empirical distribution, SGPO guarantees a mere $\mathcal{O}(\epsilon)$ penalty in regret, thereby remaining robust under moderate annotation noise or distribution shift. Moreover, whereas DPO’s regret can grow linearly with the magnitude of the shift, SGPO constrains worst-case losses even in adversarial scenarios. Finally, by treating preference alignment as a robust \min_P optimization, SGPO can mitigate *mismatches between labeled and unlabeled sets*, making it particularly appealing when human annotations are scarce or must be supplemented by self-annotation. Altogether, these properties form the theoretical foundation for the practical algorithm described next (Section 3).

3. Practical Instantiation: SSAPO Algorithm

We now present a *practical* and *computationally tractable* realization of SGPO, called *Stackelberg Self-Annotated Preference Optimization (SSAPO)*. This method approximates the iterative leader–follower updates of Theorem 2.3 and Eqs. (8)–(9), overcoming three major challenges in realistic preference alignment:

1. *Minimal Human Labels via Self-Annotation.* We begin with a small “seed” of human-labeled preferences and augment the dataset by letting the *current policy* rank its own responses on unlabeled prompts.
2. *Convexity/Concavity Mismatch.* When the function $\ell(\cdot)$ is *concave*, the DRO literature [Mohajerin Esfahani & Kuhn \(2018\)](#) provides a finite-dimensional max-form program that solves the follower update. However $\ell(\xi) = -\log \sigma(\xi)$ is convex in ξ . We therefore approximate $\ell(\xi)$ by a piecewise-linear *concave* function.
3. *Scalability via Uniform Grouping.* For large-scale datasets (potentially hundreds of thousands of preferences), we split the data into subsets and solve each subset’s robust problem in parallel, then merge solutions to form an adversarial P^* for the entire set.

Below, we restate the relevant DRO theorem and describe how to approximate $-\log \sigma(\xi)$ by a concave, piecewise-linear function for solving the follower update (Section 3.1). We then detail how SSAPO’s leader–follower loop integrates *self-annotation* and *uniform grouping* (Section 3.2), and finally discuss the impact of these approximations on SGPO’s theoretical guarantees.

3.1. Solving the Follower’s Update with DRO

3.1.1. CONSTRUCT WORST-CASE DISTRIBUTION

Consider the distributionally robust problem

$$\sup_{P \in B_\epsilon(\hat{P}_N)} \mathbb{E}_P [\ell(\xi)],$$

$$\hat{P}_N = \frac{1}{N} \sum_{i=1}^N \delta_{\hat{\xi}_i}, B_\epsilon(\hat{P}_N) = \left\{ P : W(P, \hat{P}_N) \leq \epsilon \right\}.$$

[Mohajerin Esfahani & Kuhn \(2018\)](#) show that if $\ell(\xi)$ is *concave*, then $\sup_P \mathbb{E}_P [\ell(\xi)]$ admits a *finite convex program* in the variables $\{\alpha_{ik}, q_{ik}\}$ whose solution yields a worst-case *extremal distribution* $P^* \in B_\epsilon(\hat{P}_N)$. Conceptually, each original sample $\hat{\xi}_i$ can “shift” by q_{ik}/α_{ik} subject to $\ell(\cdot)$ being evaluated at $\hat{\xi}_i - (q_{ik}/\alpha_{ik})$. In the max-form, that shift tries to *increase* $\ell(\xi)$ in a worst-case sense. Formally,

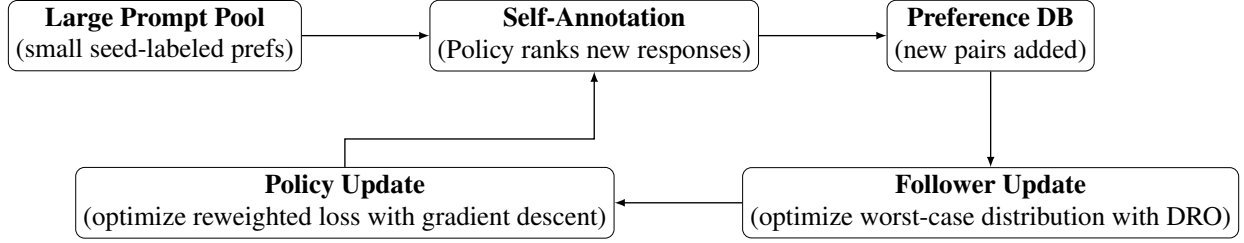


Figure 1. SSAPO workflow. We maintain a large prompt pool and a small set of seed-labeled preferences. The policy self-annotates new prompts by generating and ranking responses, thus expanding the preference database. A follower then identifies a worst-case distribution for these preferences, and the leader (policy) is updated accordingly. This process repeats for multiple iterations.

Theorem 3.1 (Worst-Case Extremal Distributions, specialized from Theorem 4.4 in Mohajerin Esfahani & Kuhn, 2018). *If $\ell(\cdot)$ is proper, concave, and lower semicontinuous on $\Xi \subset \mathbb{R}^m$, then*

$$\sup_{P \in B_\epsilon(\hat{P}_N)} \mathbb{E}_P [\ell(\xi)] = \max_{\substack{\alpha_{ik}, q_{ik} \\ i=1, \dots, N; k=1, \dots, K}} \frac{1}{N} \sum_{i=1}^N \sum_{k=1}^K \alpha_{ik} \ell\left(\hat{\xi}_i - \frac{q_{ik}}{\alpha_{ik}}\right)$$

subject to the usual Wasserstein and feasibility constraints $\frac{1}{N} \sum_{i,k} \|q_{ik}\| \leq \epsilon$, $\sum_k \alpha_{ik} = 1$, $\alpha_{ik} \geq 0$, and $\hat{\xi}_i - \frac{q_{ik}}{\alpha_{ik}} \in \Xi$. A discrete distribution $\frac{1}{N} \sum_{i,k} \alpha_{ik} \delta_{\hat{\xi}_i - \frac{q_{ik}}{\alpha_{ik}}}$ achieves the supremum, thus providing $P^* \in B_\epsilon(\hat{P}_N)$.

Since $\ell(\xi) = -\log \sigma(\xi)$ is actually *convex* rather than concave, we cannot directly apply Theorem 3.1. Hence, Section 3.1.2 explains how to construct a concave *piecewise-linear* under-approximation $\tilde{\ell}(\cdot) \leq -\log \sigma(\cdot)$, enabling us to adopt the same finite convex program framework.

3.1.2. CONCAVE PIECEWISE-LINEAR APPROXIMATION

To embed our $\ell(\xi) = -\log \sigma(\xi)$ into Theorem 3.1, we construct a *concave under-approximation* $\tilde{\ell}(\xi)$ represented by K linear pieces:

$$\tilde{\ell}(\xi) = \max_{1 \leq k \leq K} \ell_k(\xi), \quad (16)$$

where each $\ell_k(\xi)$ is an affine function, and $\forall \xi : \tilde{\ell}(\xi) \leq -\log \sigma(\xi)$. Because the $\ell_k(\cdot)$ are linear and we take a max, $\tilde{\ell}(\cdot)$ is indeed a *concave*, piecewise-linear function.

One practical construction is to partition an interval of interest into K “knots” $\{\xi^{(k)}\}$ and define $\ell_k(\xi)$ as the tangent line *from below* (or a chord) such that $\ell_k(\xi^{(k)}) = -\log \sigma(\xi^{(k)})$ but $\ell_k(\xi) \leq -\log \sigma(\xi)$ for all ξ in the domain. Equidistant points can be taken in the interval $[0, 1]$, considering the image of sigmoid activations $\sigma(\cdot)$ is $[0, 1]$.

Follower’s DRO Problem with $\tilde{\ell}(\cdot)$. Replacing $\ell(\xi)$ in Theorem 3.1 with $\tilde{\ell}(\xi)$ gives a *finite convex program* that yields $P^* \in B_\epsilon(\hat{P}_N)$. Concretely,

$$\max_{P \in B_\epsilon(\hat{P}_N)} \mathbb{E}_P [\tilde{\ell}(\xi)] = \max_{\{\alpha_{ik}, q_{ik}\}} \frac{1}{N} \sum_{i=1}^N \sum_{k=1}^K \alpha_{ik} \ell_k\left(\hat{\xi}_i - \frac{q_{ik}}{\alpha_{ik}}\right), \quad (17)$$

subject to standard Wasserstein constraints. Since $\tilde{\ell}(\xi) \leq -\log \sigma(\xi)$, this *under-approximation* yields a P^* that is valid—but *less adversarial*—for the original $\ell(\xi)$.

3.2. SSAPO: Algorithmic Steps

Figure 1 summarizes the SSAPO workflow. Starting with a small seed of human-labeled preferences plus a large unlabeled pool, we proceed in the following loop:

1. *Self-Annotation.* At each iteration, we sample new unlabeled prompts from $\mathcal{D}_{\text{unlabeled}}$ and let the current policy π_{θ_t} generate candidate responses. The policy *ranks* them to form winner-loser pairs (y_w, y_l) , which expand the preference dataset \mathcal{D} . From these, we build $\hat{\xi}_i = R_{\theta_t}(y_w^i) - R_{\theta_t}(y_l^i)$.

2. *Concave Piecewise-Linear Approx.* We fix K and define $\{\ell_k\}_{k=1}^K$ such that $\tilde{\ell}(\xi) = \max_k \ell_k(\xi) \leq -\log \sigma(\xi)$ (as in Eq. (16)).
3. *Worst-Case Distribution.* We form $\hat{P}_N = \frac{1}{N} \sum_{i=1}^N \delta_{\hat{\xi}_i}$, then solve Eq. (17) with $\tilde{\ell}$. By Theorem 3.1, the solution is a discrete distribution $P_t^* \in B_\epsilon(\hat{P}_N)$ that shifts each $\hat{\xi}_i$ by up to q_{ik}^*/α_{ik}^* , then applies the affine $\ell_k(\cdot)$ and weights α_{ik}^* .
4. *Policy Update.* We train π_θ on P_t^* by minimizing $\mathbb{E}_{P_t^*}[-\log \sigma(R_\theta(y_w) - R_\theta(y_t))]$. Noting that P_t^* identifies how often each shifted ξ_i is “activated,” we can equivalently reweight the original samples for gradient-based updates.

Repeating for T total iterations yields the final aligned policy π_{θ_T} . A more explicit version of SSAPO is provided in Algorithm 1 (Appendix E), along with its computational complexity analysis.

3.2.1. SCALABILITY VIA UNIFORM GROUPING AND APPROXIMATION

Grouping Large Datasets. When N is large (e.g. 10^5 or more preferences), solving the convex program in Step (Worst-Case Distribution) can be expensive. A popular heuristic partitions $\{\hat{\xi}_1, \dots, \hat{\xi}_N\}$ into M groups (each of size $G = N/M$), and solves the finite program (17) separately within each group. The resulting distributions P_m^* are then averaged (or merged proportionally):

$$P_{\text{final}}^* = \frac{1}{M} \sum_{m=1}^M P_m^*.$$

While not an *exact* solution to the global N -sample problem, this still confers substantial robustness while reducing complexity from N to $G \ll N$ in each subproblem. In summary, this grouping approach greatly reduces memory/compute cost, and is parallelizable.

Remark 3.2 (Approximation Effects on SGPO Guarantees). Two approximations separate SSAPO from the ideal solution of Section 2: (1) *Concave Under-Approximation*: Replacing $-\log \sigma(\cdot)$ with its piecewise-linear approximation $\tilde{\ell}(\cdot)$ (i.e., $\tilde{\ell}(\xi) \leq -\log \sigma(\xi)$) ensures feasibility in Theorem 3.1, but slightly weakens the adversarial effect. Consequently, the policy may be *less robust* than in the fully ideal solution $\max_P \mathbb{E}_P[-\log \sigma(\cdot)]$. Increasing K (i.e., refining the linear approximation) narrows this gap. (2) *Partitioned Solver*: Rather than solving one global $\arg \max_{P \in B_\epsilon(\hat{P}_N)}$, SSAPO partitions the dataset into M groups and separately solves M subproblems. Merging their solutions may deviate from a unified optimum, but it still explores adversarial reweighting in each subgroup, preserving much of SGPO’s robustness against distributional shifts. Despite these approximations, SSAPO preserves the *Stackelberg* essence: the policy is trained against worst-case reweightings within an ϵ -Wasserstein distance. As a result, it retains the key benefit of *bounded regret* for moderate shifts (Theorem 2.5), while remaining computationally tractable. Indeed, if $K \rightarrow \infty$ and $M = 1$, SSAPO recovers the exact follower solution (subject to sampling). Empirically (Section 4), these approximations still yield substantial label-efficiency and robustness gains over standard DPO.

4. Experiments

In this section, we present an extensive empirical evaluation of our proposed *Stackelberg Self-Annotated Preference Optimization* (SSAPO) algorithm.

4.1. Experiment Setup

We introduce the basic experiment setup in this subsection (Cf. Appendix F for more details). The settings are mostly consistent to the recent literature [Kim et al. \(2025\)](#). **Datasets.** We used the UltraFeedback dataset ([Cui et al., 2023](#)), containing 60K samples. A seed of 2K human-labeled preferences (3.3% of total data) was used for initial training. The rest (58K samples) were split into three subsets (8K, 20K, and 30K) for self-annotation in iterative stages.

Models. We use the supervised fine-tuned Mistral-7B-0.1 ([Jiang et al., 2023a](#)) as the initial model π_{init} and LLaMA-3-8B³ for compatibility checks. All models are fine-tuned on UltraChat ([Ding et al., 2023](#)).

Evaluations. We use **AlpacaEval 2.0** ([Dubois et al., 2024a](#)) for instruction-following tasks and **MT-Bench** ([Zheng et al., 2023](#)) to evaluate multi-turn performance across tasks like math, coding, and writing. Both benchmarks assess the alignment with human preferences and the model’s functional proficiency. We stress that AlpacaEval 2.0 is especially useful for measuring how well the model aligns with general user preferences (and controlling for length bias), whereas MT-Bench

³[meta-llama/Meta-Llama-3-8B-Instruct](#)

tests the model’s functional capabilities across a broader range of tasks.

Implementation. We initialize training with DPO on 2K seed samples, followed by 3 iterative stages of self-annotation. In each stage, new preferences are generated via a policy that ranks response pairs. A distributionally robust optimization (DRO) is performed using sequential least squares programming (SLSQP) to adjust the model based on adversarial shifts within a Wasserstein ball. The group size G for parallel computation is set to 100 unless otherwise specified.

Baselines. We consider the following baselines for comparison: (1) DPO, which performs DPO training only on the seed data. (2) Iter DPO (Xiong et al., 2024), which iteratively generates preference data using an external reward model (PairRM) (Jiang et al., 2023b) or LLM-as-judge (Li et al., 2024). (3) SPA (Kim et al., 2025), which iteratively generates preference data using implicit reward model.

Table 1. Main results. Evaluation results on AlpacaEval 2.0 and MT-Bench with different variants of Mistral-7B-v0.1 and LLaMA3-8B. All models use the same 3.3% preference data with gold label as seed data. The best and second-best results are highlighted in bold and underlined, respectively. Most of the baseline results are from (Kim et al., 2025).

Models	AlpacaEval 2.0		MT-Bench
	Len-control. Win Rate (%)	Win Rate vs. GPT-4 (%)	Avg. Score (0-10)
Mistral-7B-DPO	9.03	7.68	6.81
Mistral-7B-Iter DPO (PairRM)	11.87	9.46	6.98
Mistral-7B-Iter DPO (LLM-as-judge)	9.28	9.18	6.67
Llama3-8B-DPO	20.61	18.04	-
Mistral-7B-SPA	15.39	21.13	6.94
Llama3-8B-SPA	21.85	24.95	7.86
Mistral-7B-SSAPO (Ours)	<u>24.44</u>	<u>35.82</u>	6.68
Llama3-8B-SSAPO (Ours)	33.33	40.12	8.03

Table 2. Comparison with different variants of Mistral. Evaluation results on AlpacaEval 2.0 and MT-Bench with different variants of Mistral-7B-v0.1. The best scores are highlighted with bold. The baseline results are from (Kim et al., 2025) and (Dubois et al., 2024b).

Models	Gold Label (%)	AlpacaEval 2.0		MT-Bench
		Len-control. Win Rate (%)	Win Rate vs. GPT-4 (%)	Avg. Score (0-10)
Mistral-7B-v0.1	-	0.17	0.50	3.25
Zephyr-7B- β	100	11.75	10.03	6.87
Mistral-7B-SFT	-	7.58	4.72	6.34
Mistral-7B-DPO	3.3	9.03	7.68	6.81
Mistral-Large (123B)	-	21.4	32.7	-
Mistral-7B-SSAPO (Ours)	3.3	24.44	35.82	6.68

4.2. Main Results

Table 1 summarizes our primary comparison on **AlpacaEval 2.0** and **MT-Bench**. All models in this comparison use only 3.3% of the UltraFeedback dataset as seed data (2K human-labeled preference pairs), with the remainder self-annotated. Our **SSAPO** method consistently outperforms DPO and other iterative baselines (e.g., Iter-DPO, SPA) in both the length-controlled (LC) and raw win-rate metrics on AlpacaEval 2.0. For Mistral-7B, **SSAPO** achieves 24.44% LC win rate and 35.82% raw win rate, compared to only 9.03% and 7.68% with standard DPO. On the larger LLaMA-3-8B model, SSAPO reaches a **33.33%** LC win rate and **40.12%** raw win rate, surpassing its SPA counterpart by a wide margin. MT-Bench scores corroborate these improvements, indicating that SSAPO yields robust, high-quality responses across diverse tasks.

To further illustrate SSAPO’s data-efficiency and robustness, Table 2 compares various Mistral models, including *Mistral-7B-SFT*, *Mistral-Large* (the number of parameters is 123B), and a fully-finetuned *Zephyr-7B- β* variant with 100% labeled data. Remarkably, **Mistral-7B-SSAPO** outperforms or closely approaches these stronger references in AlpacaEval 2.0, despite using only 3.3% of the human-labeled training set. This demonstrates that *a principled Stackelberg method can substantially mitigate the reliance on massive human annotations*. It also aligns with our theoretical findings (Section 2) that

SGPO-based approaches, when instantiated as SSAPO, achieve bounded regret under moderate preference shift.

4.3. Ablation and Sensitivity Analysis

Table 3. Effect of Wasserstein Radius ϵ on Performance. Evaluation results on Mistral-7B, showing the impact of varying the Wasserstein radius on the Len-control. Win Rate and Win Rate vs. GPT-4.

ϵ	0	0.01	0.03	0.05	0.1
Len-control. Win Rate (%)	19.76	24.44	22.42	23.20	19.78
Win Rate vs. GPT-4 (%)	26.58	35.82	32.30	32.92	25.84

Table 4. Impact of Tangent Size on Model Performance. Evaluation results on Mistral-7B, showing the effect of the number of tangents K in the piecewise-linear approximation.

K	5	6	7
Len-control. Win Rate (%)	22.89	23.20	19.05
Win Rate vs. GPT-4 (%)	29.19	32.92	25.84

Table 5. Effect of Group Size on Performance. Evaluation results on Mistral-7B, showing how different group sizes G impact the runtime and model performance.

G	100	200	300
CPU Runtime (min)	45	206	630
Len-control. Win Rate (%)	13.70	14.81	16.95
Win Rate vs. GPT-4 (%)	10.00	11.74	14.91

We conduct a series of ablation studies to understand the factors influencing the efficacy and robustness of our *Stackelberg Self-Annotated Preference Optimization* (SSAPO). Specifically, we vary the Wasserstein radius ϵ , the number of tangents K , the group size G , and the size/iteration of seed data. We conduct the experiments on the Mistral-7B model for budget consideration. These experiments confirm our method’s flexibility and validate the practical design choices guided by our theoretical framework.

Wasserstein Radius ϵ . Table 3 demonstrates how model performance changes with different Wasserstein radius. When $\epsilon = 0$, our approach reduces to self-annotated DPO without robust reweighting, yielding weaker results (19.76% LC win rate). As ϵ increases slightly (e.g., 0.01–0.05), both win-rates improve substantially, with the best outcomes at $\epsilon = 0.01$. However, overly large ϵ (e.g., 0.1) can make the adversarial shift too pessimistic, degrading performance. These findings align with our theoretical analysis in Section 2, where moderate ϵ provides a robust yet not overly conservative solution, thus striking the optimal balance between data fidelity and adversarial resilience.

Number of Tangents K . Since our piecewise-linear approximation of $-\log \sigma(\cdot)$ uses K linear segments (cf. Section 3), we examine how varying K affects alignment (Table 4). At $K = 5$, the model attains a 22.89% LC win-rate, while increasing to $K = 6$ yields a marginally better 23.20%. Interestingly, moving to $K = 7$ leads to performance drops (19.05%). We hypothesize that while a larger K refines the concave envelope, it may also overcomplicate optimization or amplify minor errors in the approximation. Thus, $K = 6$ serves as a sweet spot in our setting, balancing expressiveness and computational stability.

Group Size G . Our distributionally robust optimization solver randomly partition data into groups of size G for parallel subproblem solutions. Table 5 illustrates the trade-off between computational cost and performance. A small group size ($G = 100$) has faster runtime (45 min) but yields a 13.70% LC win-rate, whereas a larger $G = 300$ reaches 16.95% yet takes over 10 times longer (630 min). This confirms that while bigger groups permit more fine-grained reweighting and hence improved alignment, the overhead grows significantly. In practice, we choose $G = 100$ or $G = 200$ for an acceptable performance–efficiency balance.

Table 6. Impact of Seed Data on Model Performance. Evaluation results on Mistral-7B, showing the effect of varying the seed data used in the iterative self-annotation process.

Seed Data	1st	2nd	3rd
Len-control. Win Rate (%)	22.43	23.20	23.75
Win Rate vs. GPT-4 (%)	29.10	32.92	24.47
Average Length	2648	3416	2121

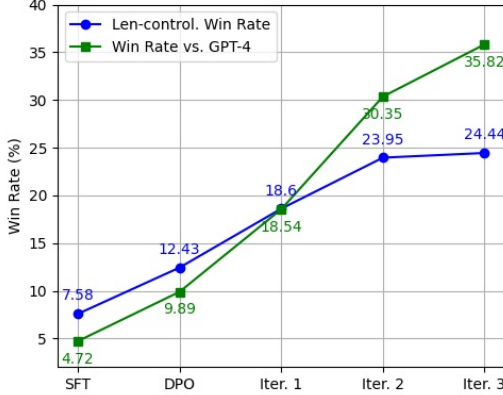


Figure 2. Improvement during iterations Evaluation results on Alpaca Eval 2.0 of initial DPO stage and each iterations, the results of the SFT model are from (Kim et al., 2025)

4.3.1. SEED DATA AND ITERATIVE SELF-ANNOTATION

Finally, Table 6 examines the influence of different seed data on Mistral-7B’s final performance after three rounds of SSAPO. We can see that the results fluctuates across seed data. We hypothesis that the fluctuation is caused by the radius parameter ϵ , which is not tuned with respect to new seed data. The radius describes the magnitude of our faith of distributional shift. A fixed radius may not truly reflect the dynamics of distribution shifts during iterations. For future work, one may consider develop an adaptive strategy for ϵ . Though we have witnessed some fluctuations, our SAPPO consistently improve upon its rival DPO and SPA across different seed data.

Iterative Performance Gains. Figure 2 provides a more direct illustration of iterative improvement over three rounds of SSAPO. Starting from a baseline DPO model, each round not only adds new self-annotated preferences but also reweights them adversarially within an ϵ -Wasserstein ball. We observe a consistent upward trend in alignment metrics during the first two rounds, validating our claim that *robust self-annotation can compensate for scarce human labels while preserving alignment quality*.

Taken together, these ablations highlight the flexibility and effectiveness of SSAPO: Moderate ϵ balances robustness and data fidelity, confirming our theoretical finding that worst-case reweighting within a bounded radius can significantly enhance alignment without over-penalizing feasible distributions. Piecewise-linear approximations with small K are sufficient to capture the shape of $-\log(\sigma(\cdot))$, maintaining computational tractability. Group size G offers a controllable trade-off between runtime and fine-grained adversarial reweighting, making the approach scalable to different budget constraints. Iterative self-annotation with minimal seed data substantially boosts alignment, demonstrating that only 2K human-labeled preferences can suffice to achieve high performance. Overall, these experiments affirm our primary contributions: a *data-efficient* and *theoretically grounded* approach to preference alignment.

5. Limitation, Future Work and Conclusion

Aiming at a data-efficient alignment method, we have introduced SGPO alignment framework with $\mathcal{O}(\epsilon)$ -bounded regret under moderate noise or distribution shifts. Our practical instantiation, SSAPO, uses self-annotation and distributionally

robust reweighting to achieve strong performance with far fewer human labels. The scalability bottleneck of SSAPO comes from the number of preferences N , we use a simple uniform group trick to balance between robustness and complexity. For further improvement, one may resort to primal-dual or specialized cutting-plane methods (Mohajerin Esfahani & Kuhn, 2018), or use approximate relaxations with entropic regularization (Cuturi, 2013). We consider a preference data restricted scenario in this paper, however, as a self-annotation procedure, SSAPO can also be integrated with prompt-generation procedure such as EVA (Ye et al., 2024), which could be crucial to scaling large language model based intelligence, considering that high-quality human data is projected to run out in the next few years (Villalobos et al., 2024).

Impact Statement

Our work aims to improve the data efficiency and robustness of language model alignment by formulating preference optimization as a Stackelberg game and introducing a self-annotation mechanism. By reducing reliance on large-scale human-labeled data, our framework could democratize alignment research and make it more accessible to smaller organizations, labs, and communities (those lack substantial annotation budgets). Moreover, robust optimization against noisy or adversarial preference distributions may help mitigate unintentional bias if the seed data deviate from the true user preference distribution.

References

Achiam, J., Adler, S., Agarwal, S., Ahmad, L., Akkaya, I., Aleman, F. L., Almeida, D., Altenschmidt, J., Altman, S., Anadkat, S., et al. Gpt-4 technical report. *arXiv preprint arXiv:2303.08774*, 2023.

Azar, M. G., Guo, Z. D., Piot, B., Munos, R., Rowland, M., Valko, M., and Calandriello, D. A general theoretical paradigm to understand learning from human preferences. In *International Conference on Artificial Intelligence and Statistics*, pp. 4447–4455. PMLR, 2024.

Bai, Y., Jones, A., Ndousse, K., Askell, A., Chen, A., DasSarma, N., Drain, D., Fort, S., Ganguli, D., Henighan, T., et al. Training a helpful and harmless assistant with reinforcement learning from human feedback. *arXiv preprint arXiv:2204.05862*, 2022.

Başar, T. and Olsder, G. J. *Dynamic noncooperative game theory*. SIAM, 1998.

Casper, S., Davies, X., Shi, C., Gilbert, T. K., Scheurer, J., Rando, J., Freedman, R., Korbak, T., Lindner, D., Freire, P., et al. Open problems and fundamental limitations of reinforcement learning from human feedback. *arXiv preprint arXiv:2307.15217*, 2023.

Chen, Z., Deng, Y., Yuan, H., Ji, K., and Gu, Q. Self-play fine-tuning converts weak language models to strong language models. In *Proceedings of the Forty-first International Conference on Machine Learning*, 2024.

Cheng, P., Yang, Y., Li, J., Dai, Y., and Du, N. Adversarial preference optimization. *arXiv preprint arXiv:2311.08045*, 2023.

Chowdhury, S. R., Kini, A., and Natarajan, N. Provably robust dpo: Aligning language models with noisy feedback. In *Proceedings of the Forty-first International Conference on Machine Learning*, 2024.

Christiano, P. F., Leike, J., Brown, T., Martic, M., Legg, S., and Amodei, D. Deep reinforcement learning from human preferences. *Advances in neural information processing systems*, 30, 2017.

Cui, G., Yuan, L., Ding, N., Yao, G., Zhu, W., Ni, Y., Xie, G., Liu, Z., and Sun, M. Ultrafeedback: Boosting language models with high-quality feedback. 2023.

Cuturi, M. Sinkhorn distances: Lightspeed computation of optimal transport. *Advances in Neural Information Processing Systems*, 26, 2013.

Ding, N., Chen, Y., Xu, B., Qin, Y., Zheng, Z., Hu, S., Liu, Z., Sun, M., and Zhou, B. Enhancing chat language models by scaling high-quality instructional conversations. *arXiv preprint arXiv:2305.14233*, 2023.

Dubois, Y., Li, C. X., Taori, R., Zhang, T., Gulrajani, I., Ba, J., Guestrin, C., Liang, P. S., and Hashimoto, T. B. Alpacafarm: A simulation framework for methods that learn from human feedback. *Advances in Neural Information Processing Systems*, 36, 2024a.

Dubois, Y., Liang, P., and Hashimoto, T. Length-controlled alpacaeval: A simple debiasing of automatic evaluators. In *First Conference on Language Modeling*, 2024b.

Ethayarajh, K., Xu, W., Muennighoff, N., Jurafsky, D., and Kiela, D. Kto: Model alignment as prospect theoretic optimization. *arXiv preprint arXiv:2402.01306*, 2024.

Hong, J., Lee, N., and Thorne, J. Orpo: Monolithic preference optimization without reference model. In *Proceedings of the 2024 Conference on Empirical Methods in Natural Language Processing*, pp. 11170–11189, 2024.

Jiang, A. Q., Sablayrolles, A., Mensch, A., Bamford, C., Chaplot, D. S., Casas, D. d. l., Bressand, F., Lengyel, G., Lample, G., Saulnier, L., et al. Mistral 7b. *arXiv preprint arXiv:2310.06825*, 2023a.

Jiang, D., Ren, X., and Lin, B. Y. Llm-blender: Ensembling large language models with pairwise ranking and generative fusion. In *The 61st Annual Meeting Of The Association For Computational Linguistics*, 2023b.

Kim, D., Lee, K., Shin, J., and Kim, J. Spread preference annotation: Direct preference judgment for efficient llm alignment. In *The Thirteenth International Conference on Learning Representations*, 2025.

Lee, H., Phatale, S., Mansoor, H., Mesnard, T., Ferret, J., Lu, K. R., Bishop, C., Hall, E., Carbune, V., Rastogi, A., et al. Rlaif vs. rlhf: Scaling reinforcement learning from human feedback with ai feedback. In *Proceedings of the Forty-first International Conference on Machine Learning*, 2024.

Li, H., Dong, Q., Chen, J., Su, H., Zhou, Y., Ai, Q., Ye, Z., and Liu, Y. Llms-as-judges: A comprehensive survey on llm-based evaluation methods. *arXiv preprint arXiv:2412.05579*, 2024.

Makar-Limanov, J., Prakash, A., Goktas, D., Ayanian, N., and Greenwald, A. Sta-rlhf: Stackelberg aligned reinforcement learning with human feedback. In *Coordination and Cooperation for Multi-Agent Reinforcement Learning Methods Workshop*, 2024.

Melnyk, I., Mroueh, Y., Belgodere, B., Rigotti, M., Nitsure, A., Yurochkin, M., Greenwald, K., Navratil, J., and Ross, J. Distributional preference alignment of llms via optimal transport. *Advances in Neural Information Processing Systems*, 2024.

Meng, Y., Xia, M., and Chen, D. Simpo: Simple preference optimization with a reference-free reward. *arXiv preprint arXiv:2405.14734*, 2024.

Mohajerin Esfahani, P. and Kuhn, D. Data-driven distributionally robust optimization using the wasserstein metric: Performance guarantees and tractable reformulations. *Mathematical Programming*, 171(1):115–166, 2018.

Munos, R., Valko, M., Calandriello, D., Azar, M. G., Rowland, M., Guo, Z. D., Tang, Y., Geist, M., Mesnard, T., Fiegel, C., et al. Nash learning from human feedback. In *Proceedings of the Forty-first International Conference on Machine Learning*, 2024.

Ouyang, L., Wu, J., Jiang, X., Almeida, D., Wainwright, C., Mishkin, P., Zhang, C., Agarwal, S., Slama, K., Ray, A., et al. Training language models to follow instructions with human feedback. *Advances in Neural Information Processing Systems*, 35:27730–27744, 2022.

Rafailov, R., Sharma, A., Mitchell, E., Manning, C. D., Ermon, S., and Finn, C. Direct preference optimization: Your language model is secretly a reward model. *Advances in Neural Information Processing Systems*, 36, 2023.

Rosset, C., Cheng, C.-A., Mitra, A., Santacroce, M., Awadallah, A., and Xie, T. Direct nash optimization: Teaching language models to self-improve with general preferences. *arXiv preprint arXiv:2404.03715*, 2024.

Sion, M. On general minimax theorems. *Pacific J. Math.*, 8(4):171–176, 1958.

Swamy, G., Dann, C., Kidambi, R., Wu, Z. S., and Agarwal, A. A minimaximalist approach to reinforcement learning from human feedback. In *Proceedings of the Forty-first International Conference on Machine Learning*, 2024.

Tunstall, L., Beeching, E., Lambert, N., Rajani, N., Rasul, K., Belkada, Y., Huang, S., von Werra, L., Fourrier, C., Habib, N., et al. Zephyr: Direct distillation of lm alignment. *arXiv preprint arXiv:2310.16944*, 2023.

Villalobos, P., Ho, A., Sevilla, J., Besiroglu, T., Heim, L., and Hobbhahn, M. Will we run out of data? limits of llm scaling based on human-generated data. *arXiv preprint arXiv:2211.04325*, pp. 13–29, 2024.

Villani, C. et al. *Optimal transport: old and new*, volume 338. Springer, 2009.

Wang, Y., Ivison, H., Dasigi, P., Hessel, J., Khot, T., Chandu, K., Wadden, D., MacMillan, K., Smith, N. A., Beltagy, I., et al. How far can camels go? exploring the state of instruction tuning on open resources. *Advances in Neural Information Processing Systems*, 36:74764–74786, 2023.

Wu, J., Xie, Y., Yang, Z., Wu, J., Chen, J., Gao, J., Ding, B., Wang, X., and He, X. Towards robust alignment of language models: Distributionally robustifying direct preference optimization. *arXiv preprint arXiv:2407.07880*, 2024a.

Wu, Y., Sun, Z., Yuan, H., Ji, K., Yang, Y., and Gu, Q. Self-play preference optimization for language model alignment. *arXiv preprint arXiv:2405.00675*, 2024b.

Xiong, W., Dong, H., Ye, C., Wang, Z., Zhong, H., Ji, H., Jiang, N., and Zhang, T. Iterative preference learning from human feedback: Bridging theory and practice for rlhf under kl-constraint. In *Proceedings of the Forty-first International Conference on Machine Learning*, 2024.

Ye, Z., Agarwal, R., Liu, T., Joshi, R., Velury, S., Le, Q. V., Tan, Q., and Liu, Y. Evolving alignment via asymmetric self-play. *arXiv preprint arXiv:2411.00062*, 2024.

Yuan, W., Pang, R. Y., Cho, K., Li, X., Sukhbaatar, S., Xu, J., and Weston, J. E. Self-rewarding language models. In *Proceedings of the Forty-first International Conference on Machine Learning*, 2024.

Zhang, Y., Yu, D., Peng, B., Song, L., Tian, Y., Huo, M., Jiang, N., Mi, H., and Yu, D. Iterative nash policy optimization: Aligning llms with general preferences via no-regret learning. In *The Thirteenth International Conference on Learning Representations*, 2025.

Zheng, L., Chiang, W.-L., Sheng, Y., Zhuang, S., Wu, Z., Zhuang, Y., Lin, Z., Li, Z., Li, D., Xing, E., et al. Judging llm-as-a-judge with mt-bench and chatbot arena. *Advances in Neural Information Processing Systems*, 36:46595–46623, 2023.

Ziegler, D. M., Stiennon, N., Wu, J., Brown, T. B., Radford, A., Amodei, D., Christiano, P., and Irving, G. Fine-tuning language models from human preferences. *arXiv preprint arXiv:1909.08593*, 2019.

Organization of the Appendix.

- **Section A** recap LLM alignment and data-efficient methods, as well as the Game-theoretic alignment methods. And discuss the connection and distinction between SGPO/SSAPO with them.
- **Section B** revisits the core definitions and properties of the 1-Wasserstein metric, including a statement of the Kantorovich–Rubinstein duality.
- **Section C** restates and discusses the regularity conditions needed for our theoretical guarantees, such as compactness and Lipschitz continuity.
- **Section D** provides detailed proofs for the existence and convergence of the Stackelberg equilibrium, as well as the regret bounds for SGPO and comparisons with DPO.
- **Section E** presents the SSAPO algorithm in pseudocode and includes an analysis of its computational complexity.
- **Section F** gives supplementary information on experimental setups, hyperparameter choices, grouping strategies for DRO, and other implementation details.
- **Section G** illustrates additional qualitative comparisons of model outputs, highlighting the differences between DPO, SPA, and SSAPO in practice.

A. More Detailed Related Work

LLM Alignment and Data-Efficient Methods Aligning large language models (LLMs) with human preferences is central to modern deployments (Ziegler et al., 2019; Ouyang et al., 2022; Bai et al., 2022). While Reinforcement Learning with Human Feedback (RLHF) (Christiano et al., 2017) trains a reward model and then maximizes it under KL constraints, it typically requires massive human-annotated data. Recent alternatives focus on *directly* fine-tuning LLMs from pairwise preference data without an explicit reward model. Notably, Direct Preference Optimization (DPO) (Rafailov et al., 2023) derives a closed-form surrogate objective that recovers RLHF’s solution but avoids a separate reward modeling stage. Subsequent works simplify or extend this pipeline; for instance, Ethayarajh et al. (2024) remove the need for pairwise labels by adopting a human utility model, while there are also works (Meng et al., 2024; Hong et al., 2024; Azar et al., 2024) introduce novel optimization objectives to handle different preference formats. Despite progress, these approaches still rely on large-scale preference annotations, making label-efficiency a key challenge. To reduce the reliance on expensive human labels, several methods have explored letting the LLM or an auxiliary model generate and rank unlabeled responses, thereby creating synthetic preference data (Jiang et al., 2023b; Yuan et al., 2024; Xiong et al., 2024; Kim et al., 2025). However, many of these approaches assume accessibility to a reliable well-aligned “judge”, which could be prohibitive costly in realistic scenarios. To address the cost bottleneck, Kim et al. (2025) propose a *Spread Preference Annotation* (SPA) framework that starts from a small seed of human-annotated preferences and iteratively expands the dataset by self-annotation. Our work is closely related to SPA: we replicate its experimental setup by using the same small-scale seed preferences and iterating between new response generation and preference learning. However, our *Stackelberg* perspective considers the inaccuracy of self-annotation, and explicitly defends against worst-case preference shifts. Empirically, we show that this game-theoretic *distributional* approach yields stronger label efficiency.

Game-Theoretic Alignment Methods An emerging body of work has begun to frame preference alignment of LLMs through the lens of *games*. A conceptual similar work (Makar-Limanov et al., 2024) propose *Stackelberg Alignment RLHF*. However, their nested gradient-based heuristic does not guaranteed to converge to the equilibrium. While we prove our updates for the leader and follower converge to an equilibrium. Meanwhile, Ye et al. (2024) present a framework that casts prompt-creator and solver asymmetric players in an evolving game, the differences between our work is we focus on evolving the distribution of the responses , while they focus on evolng the distribution of the prompts. SPIN (Chen et al., 2024) use self-play to iteratively refine a policy without additional human data, however they assume accessible to adequate supervised fine-tuning (SFT) data. Other works adopt *Nash* or *minimax* formulations: Melnyk et al. (2024) study alignment via an optimal-transport objective to capture distributional preferences, Zhang et al. (2025) and Rosset et al. (2024) formulate alignment as a two-player game aiming for a Nash policy, and Munos et al. (2024) proposes “Nash learning from human feedback” by treating the policy and a competing policy as iterative players. Likewise, Swamy et al. (2024); Wu et al. (2024b) introduce self-play preference optimization methods in which two policies repeatedly compete under a constant-sum setting. They demonstrate promising performance on synthetic and text-based benchmarks, but typically set both players

as *policy vs. policy*. By contrast, our *SGPO* framework focuses on *policy vs. distribution*: the leader policy maximizes preference likelihood, while the follower adversarially reweights or shifts the empirical preference distribution. This setup offers a distinct distributional robust-control view, leading to tight theoretical guarantees (e.g., $\mathcal{O}(\epsilon)$ -bounded regret) and a practical algorithm (SSAPO) that is readily integrated with self-annotation. Hence, our method complements the “policy vs. policy” family by delivering strong resistance to noisy or distribution-mismatched preferences at small annotation cost.

B. Preliminaries on the Wasserstein Metric Space

Wasserstein (or Earth Mover’s) distances are widely used in robust optimization and optimal transport to measure how far two probability distributions are from one another (Villani et al., 2009). Below, we give a concise overview of the 1-Wasserstein metric on a subset $\Xi \subseteq \mathbb{R}^m$. We also recap the Kantorovich–Rubinstein duality (Lemma B.2), which is central to several of our regret and robustness proofs in the main text.

B.1. Definition of the 1-Wasserstein Metric

Let $\mathcal{M}(\Xi)$ be the space of all probability distributions supported on Ξ such that

$$\mathbb{E}_{\xi \sim F} [\|\xi\|] = \int_{\Xi} \|\xi\| dF(\xi) < \infty.$$

In our setting, $\|\cdot\|$ can be any norm on \mathbb{R}^m , typically the Euclidean norm (although other choices are possible).

Definition B.1 (1-Wasserstein Metric). For two probability distributions $F_1, F_2 \in \mathcal{M}(\Xi)$, the *1-Wasserstein* distance (often just called “the Wasserstein distance”) is defined as

$$d(F_1, F_2) := \inf_{\pi \in \Pi(F_1, F_2)} \left\{ \int_{\Xi \times \Xi} \|\xi_1 - \xi_2\| d\pi(\xi_1, \xi_2) \right\}, \quad (18)$$

where $\Pi(F_1, F_2)$ is the set of all joint distributions on $\Xi \times \Xi$ whose marginals are F_1 and F_2 , respectively. Intuitively, π specifies how “mass” is transported from points in the support of F_1 to points in the support of F_2 , and $\|\xi_1 - \xi_2\|$ is the cost of moving a unit of mass from ξ_1 to ξ_2 .

Equivalently, one can interpret the Wasserstein distance as the minimal cost of transforming the distribution F_1 into F_2 when the cost of moving a unit mass from ξ_1 to ξ_2 is $\|\xi_1 - \xi_2\|$. This framework underpins many distributionally robust methods, including the SGPO formulation in our paper.

B.2. Kantorovich–Rubinstein Duality

A crucial result for the 1-Wasserstein distance is the Kantorovich–Rubinstein duality (Theorem 5.9 in Villani et al. (2009)), which states that the infimum over transport plans (as in Definition B.1) is equivalent to a supremum over 1-Lipschitz test functions. We use this lemma extensively to derive Lipschitz-based bounds in the main proofs (e.g., Theorems D.4–D.6).

Lemma B.2 (Kantorovich–Rubinstein Duality). *Let $F_1, F_2 \in \mathcal{M}(\Xi)$ with finite first moments. Then the 1-Wasserstein distance (18) admits the following dual representation:*

$$d(F_1, F_2) = \sup_{\|f\|_{\text{Lip}} \leq 1} (\mathbb{E}_{\xi \sim F_1} [f(\xi)] - \mathbb{E}_{\xi \sim F_2} [f(\xi)]), \quad (19)$$

where the supremum is taken over all 1-Lipschitz functions $f : \Xi \rightarrow \mathbb{R}$, i.e. functions satisfying

$$|f(\xi) - f(\xi')| \leq \|\xi - \xi'\| \quad \forall \xi, \xi' \in \Xi.$$

Lemma B.2 underpins many of our theoretical arguments, particularly in bounding the gap between performance under the empirical distribution \hat{P} and any perturbed distribution P in a Wasserstein ball $\mathcal{U}_\epsilon(\hat{P})$. As shown in Section D of our paper, it simplifies comparing $\mathbb{E}_P[f]$ and $\mathbb{E}_{\hat{P}}[f]$ when f is Lipschitz in model parameters or responses.

C. Regularity Conditions for Stackelberg Game Preference Optimization

Throughout the analysis, we require standard continuity, convexity, and compactness conditions:

Assumption C.1 (Regularity Conditions). • **Compactness.** $\Pi \subseteq \mathbb{R}^d$ is compact (or effectively constrained), $\mathcal{Y} \subseteq \mathbb{R}^m$ is bounded, and the Wasserstein ball $\mathcal{U}_\epsilon(\hat{P})$ is compact in $\mathcal{P}(\mathcal{Y} \times \mathcal{Y})$.

- **Lipschitz Continuity.** We assume : The function $R_\pi(y)$ is L_R -Lipschitz in y , uniformly for $\pi \in \Pi$. That is, $|R_\pi(y) - R_\pi(y')| \leq L_R \|y - y'\|$. The policy mapping $\theta \mapsto \pi_\theta$ is sufficiently smooth, e.g. its gradient is L_π -Lipschitz, though only a bounded-gradient property may also suffice.
- **Convexity.** The set $\mathcal{U}_\epsilon(\hat{P})$ is convex in the space of probability measures with respect to the Wasserstein metric, consistent with standard definitions of Wasserstein balls (Villani et al., 2009; Mohajerin Esfahani & Kuhn, 2018).

Remark C.2 (Bounded Domain for Neural Networks). Although neural network parameters $\theta \in \mathbb{R}^d$ are technically unbounded, many theoretical analyses restrict θ to a large but bounded ball (via a norm constraint) or rely on a coercive objective to prevent unbounded parameter growth. Hence, requiring Π to be compact is common in theoretical treatments. In practice, gradient-based optimization does not typically push $\|\theta\|$ to infinity.

D. Theoretical Results

D.1. Existence and Convergence to a Stackelberg Equilibrium

Theorem D.1 (Existence of Stackelberg Equilibrium). *Under Assumption C.1, the two-player game defined by*

$$\max_{\pi \in \Pi} \min_{P \in \mathcal{U}_\epsilon(\hat{P})} J(\pi, P),$$

$$\text{where } J(\pi, P) = \mathbb{E}_P \left[\log \sigma(R_\pi(y_w) - R_\pi(y_l)) \right]$$

admits at least one Stackelberg equilibrium (π^*, P^*) .

Proof. We proof the existence by quoting the famous Sion's Minimax Theorem (Sion, 1958) as the key lemma.

Lemma D.2 (Sion's Minimax Theorem Sion (1958)). *Let X and Y be convex and compact subsets of topological vector spaces. Suppose $\phi : X \times Y \rightarrow \mathbb{R}$ is a function satisfying the following conditions:*

- For each fixed $y \in Y$, the map $x \mapsto \phi(x, y)$ is concave and upper semi-continuous in x .
- For each fixed $x \in X$, the map $y \mapsto \phi(x, y)$ is convex and lower semi-continuous in y .

Then

$$\max_{x \in X} \min_{y \in Y} \phi(x, y) = \min_{y \in Y} \max_{x \in X} \phi(x, y).$$

Step 1 (Concavity in π): Fix $P \in \mathcal{P}(\mathcal{Y} \times \mathcal{Y})$. The function

$$\pi \mapsto \log \sigma(R_\pi(y_w) - R_\pi(y_l))$$

is concave in π provided $R_\pi(y)$ is affine or at least concave in π . More precisely, if we treat $R_\pi(y)$ as a linear functional (e.g. the logit induced by π_θ), then $\log \sigma(\cdot)$ is concave in its argument. Under mild conditions (e.g. standard neural network approximation with linear final layer), the resulting composition remains concave or quasi-concave in θ .

Step 2 (Convexity in P): For a fixed π ,

$$P \mapsto \mathbb{E}_P [\log \sigma(R_\pi(y_w) - R_\pi(y_l))]$$

is linear (hence convex) in P . Indeed, $\mathbb{E}_P[\cdot]$ is always an affine operator in probability measures.

Step 3 (Compactness & Sion's Theorem): By Assumption C.1, Π is compact and $\mathcal{U}_\epsilon(\hat{P})$ is convex and compact in the Wasserstein sense. Hence, Sion's minimax theorem (Sion, 1958) applies and guarantees a saddle-point solution (π^*, P^*) . By definition, that saddle point coincides with a Stackelberg equilibrium in this setting:

$$\max_{\pi \in \Pi} \min_{P \in \mathcal{U}_\epsilon(\hat{P})} J(\pi, P) = \min_{P \in \mathcal{U}_\epsilon(\hat{P})} \max_{\pi \in \Pi} J(\pi, P).$$

Thus, an equilibrium pair exists. □

Theorem D.3 (Linear Convergence to Stackelberg Equilibrium). *Under Assumption C.1, the sequence $\{(\pi_t, P_t)\}_{t \geq 0}$ generated by the following procedure converges to the unique Stackelberg equilibrium (π^*, P^*) .*

$$\pi_{t+1} = \arg \max_{\pi \in \Pi} \min_{P \in \mathcal{U}_\epsilon(P_t)} J(\pi, P), \quad (20)$$

$$P_{t+1} = \arg \min_{P \in \mathcal{U}_\epsilon(P_t)} J(\pi_{t+1}, P), \quad (21)$$

starting from an initial pair (π_0, P_0) . Here, we shift the center of the Wasserstein ball in each iteration to P_t .

Moreover, the convergence is linear, i.e. there exists $\gamma < 1$ such that

$$\rho((\pi_{t+1}, P_{t+1}), (\pi^*, P^*)) \leq \gamma \rho((\pi_t, P_t), (\pi^*, P^*)),$$

where ρ is a suitable metric (e.g. $\rho((\pi, P), (\pi', P')) = \|\pi - \pi'\| + W(P, P')$).

Proof. **Step 1 (Policy update $\pi_t \rightarrow \pi_{t+1}$):** By definition,

$$\pi_{t+1} = \arg \max_{\pi} \min_{P \in \mathcal{U}_\epsilon(P_t)} J(\pi, P).$$

If we assume (or approximate) that $\max_{\pi} \min_{P}$ is well-approximated by a (sub)gradient-based ascent with step size η , then Lipschitz continuity in π (Assumption C.1) ensures a contraction of the form:

$$\|\pi_{t+1} - \pi_t\| \leq \gamma_\pi \|\pi_t - \pi_{t-1}\|,$$

with $\gamma_\pi < 1$ provided η is sufficiently small. (Alternatively, one can rely on standard monotone operator theory to show a unique fixed point.)

Step 2 (Distribution update $P_t \rightarrow P_{t+1}$): From (21),

$$P_{t+1} = \arg \min_{P \in \mathcal{U}_\epsilon(P_t)} J(\pi_{t+1}, P).$$

Since $J(\pi_{t+1}, P)$ is L_R -Lipschitz in the support of P , the Wasserstein-bounded set $\mathcal{U}_\epsilon(P_t)$ implies

$$W(P_{t+1}, P_t) \leq \frac{\epsilon L_R}{1 + \epsilon L_R} W(P_t, P_{t-1}),$$

yielding a contraction factor $\gamma_P = \frac{\epsilon L_R}{1 + \epsilon L_R} < 1$.

Step 3 (Combined contraction): Define $\rho((\pi, P), (\pi', P')) = \|\pi - \pi'\| + W(P, P')$. From Steps 1–2, one can show

$$\rho((\pi_{t+1}, P_{t+1}), (\pi_t, P_t)) \leq \max(\gamma_\pi, \gamma_P) \rho((\pi_t, P_t), (\pi_{t-1}, P_{t-1})).$$

Hence, by the Banach fixed-point theorem, the sequence converges linearly to a unique fixed point. That fixed point necessarily satisfies the Stackelberg equilibrium conditions (Definition 2.1). \square

D.2. Regret Analysis and Comparison between SGPO and DPO

D.2.1. SGPO's REGRET

Theorem D.4 (Worst-Case Performance Guarantee for SGPO). *Under Assumption C.1, let π^* be the SGPO solution. Then for every $P \in \mathcal{U}_\epsilon(\hat{P})$,*

$$\mathcal{P}(\pi^*, P) \geq \mathcal{P}(\pi^*, \hat{P}) - L_R \epsilon. \quad (22)$$

In other words, the performance drop from \hat{P} to any $P \in \mathcal{U}_\epsilon(\hat{P})$ is at most $L_R \epsilon$.

Proof. By the Kantorovich-Rubinstein duality in Lemma B.2, for any 1-Lipschitz function f and distributions P_1, P_2 ,

$$|\mathbb{E}_{P_1}[f] - \mathbb{E}_{P_2}[f]| \leq W(P_1, P_2).$$

Take $f(y_w, y_l) = \log \sigma(R_{\pi^*}(y_w) - R_{\pi^*}(y_l))$. By assumption, $R_{\pi^*}(\cdot)$ is L_R -Lipschitz, so we can bound the overall Lipschitz constant of f by L_R . Hence,

$$|\mathcal{P}(\pi^*, P) - \mathcal{P}(\pi^*, \hat{P})| \leq L_R W(P, \hat{P}) \leq L_R \epsilon.$$

Thus, $\mathcal{P}(\pi^*, P) \geq \mathcal{P}(\pi^*, \hat{P}) - L_R \epsilon$. \square

Regret Notation. We define the regret of a policy π on a distribution P as

$$\text{Regret}(\pi, P) = \max_{\tilde{\pi}} \mathcal{P}(\tilde{\pi}, P) - \mathcal{P}(\pi, P). \quad (23)$$

If $\pi_P^* = \arg \max_{\tilde{\pi}} \mathcal{P}(\tilde{\pi}, P)$, then $\text{Regret}(\pi, P) = \mathcal{P}(\pi_P^*, P) - \mathcal{P}(\pi, P)$.

Theorem D.5 (SGPO Regret Bound). *For the SGPO policy π^* , we have*

$$\sup_{P \in \mathcal{U}_\epsilon(\hat{P})} \text{Regret}(\pi^*, P) \leq 2 L_R \epsilon. \quad (24)$$

Thus, SGPO is robust: under any shift of at most ϵ , its regret is bounded by a constant factor of ϵ .

Proof. Let $\pi_P^* \in \arg \max_{\pi} \mathcal{P}(\pi, P)$. Then

$$\text{Regret}(\pi^*, P) = \mathcal{P}(\pi_P^*, P) - \mathcal{P}(\pi^*, P).$$

By Theorem D.4 and the triangle inequality,

$$\begin{aligned} \text{Regret}(\pi^*, P) &\leq [\mathcal{P}(\pi_P^*, \hat{P}) + L_R \epsilon] - [\mathcal{P}(\pi^*, \hat{P}) - L_R \epsilon] \\ &= [\mathcal{P}(\pi_P^*, \hat{P}) - \mathcal{P}(\pi^*, \hat{P})] + 2 L_R \epsilon. \end{aligned}$$

Since π^* is the minimax solution under \hat{P} , we have $\mathcal{P}(\pi_P^*, \hat{P}) \leq \mathcal{P}(\pi^*, \hat{P})$. Hence the bracketed term is ≤ 0 . Therefore,

$$\text{Regret}(\pi^*, P) \leq 2 L_R \epsilon.$$

Taking the supremum over $P \in \mathcal{U}_\epsilon(\hat{P})$ proves the claim. \square

D.2.2. COMPARING DPO'S REGRET

Theorem D.6 (DPO Regret Lower Bound). *Let $\pi_{\text{DPO}} = \arg \max_{\pi} \mathcal{P}(\pi, \hat{P})$, and let P^* be a distribution satisfying $W(\hat{P}, P^*) = \delta$. Then*

$$\text{Regret}(\pi_{\text{DPO}}, P^*) \geq L_R (\delta - 2\epsilon). \quad (25)$$

In particular, if $\delta \gg \epsilon$, DPO's regret grows linearly in δ .

Proof. Let $\pi_{P^*}^* \in \arg \max_{\pi} \mathcal{P}(\pi, P^*)$. Then

$$\begin{aligned} \text{Regret}(\pi_{\text{DPO}}, P^*) &= \mathcal{P}(\pi_{P^*}^*, P^*) - \mathcal{P}(\pi_{\text{DPO}}, P^*) \\ &> [\mathcal{P}(\pi_{P^*}^*, \hat{P}) - L_R \delta] - [\mathcal{P}(\pi_{\text{DPO}}, \hat{P}) + L_R \delta] \\ &= [\mathcal{P}(\pi_{P^*}^*, \hat{P}) - \mathcal{P}(\pi_{\text{DPO}}, \hat{P})] - 2 L_R \delta. \end{aligned} \quad (26)$$

Since π_{DPO} is optimal on \hat{P} , the bracketed term is ≤ 0 . Thus

$$\text{Regret}(\pi_{\text{DPO}}, P^*) \geq -2 L_R \delta.$$

However, once $\delta > 2\epsilon$, Theorem D.5 implies $\text{Regret}(\pi^*, P^*) \leq 2 L_R \epsilon < L_R \delta$. Hence

$$\text{Regret}(\pi_{\text{DPO}}, P^*) - \text{Regret}(\pi^*, P^*) \geq L_R (\delta - 2\epsilon).$$

Equivalently, $\text{Regret}(\pi_{\text{DPO}}, P^*) \geq L_R (\delta - 2\epsilon)$. \square

Corollary D.7 (SGPO Advantage Over DPO). *If $W(\hat{P}, P^*) = \delta > 2\epsilon$, then*

$$\frac{\text{Regret}(\pi_{\text{DPO}}, P^*)}{\text{Regret}(\pi^*, P^*)} \geq \frac{\delta - 2\epsilon}{2\epsilon}. \quad (27)$$

Thus, SGPO's robust policy can outperform DPO by a factor of $\frac{\delta}{2\epsilon} - 1$ under sufficiently large distribution shift δ .

Proof. The proof is straightforward following the SGPO's regret bound and the DPO's regret lower bound. \square

Algorithm 1 Stackelberg Self-Annotated Preference Optimization (SSAPO)

Require: *Seed labeled set $\mathcal{D}_{\text{seed}}$; unlabeled data $\mathcal{D}_{\text{unlabeled}}$; Wasserstein radius ϵ ; number of linear pieces K ; max iterations T .*

- 1: Initialize policy θ_0 , set $\mathcal{D} \leftarrow \mathcal{D}_{\text{seed}}$.
- 2: **for** $t = 0$ **to** $T - 1$ **do**
- 3: **(Self-Annotation):** From $\mathcal{D}_{\text{unlabeled}}$, sample prompts, generate & rank responses under π_{θ_t} , add new preference pairs (y_w, y_l) to \mathcal{D} .
- 4: **(Form \hat{P}_N):** For each $(y_w^i, y_l^i) \in \mathcal{D}$, define $\hat{\xi}_i = R_{\theta_t}(y_w^i) - R_{\theta_t}(y_l^i)$, and let $\hat{P}_N = \frac{1}{N} \sum_{i=1}^N \delta_{\hat{\xi}_i}$.
- 5: **(Concave Pieces):** Choose K linear functions $\ell_k(\cdot)$ such that $\tilde{\ell}(\xi) = \max_{1 \leq k \leq K} \ell_k(\xi) \leq -\log \sigma(\xi)$. E.g., pick K equidistant $\{\xi^{(k)}\}$ in $[0, 1]$ (or a suitable domain) and define $\ell_k(\cdot)$ to be a chord or tangent from below.
- 6: **(Worst-Case Distribution):** Solve the DRO finite convex program

$$P_t^* \in \arg \max_{P \in B_\epsilon(\hat{P}_N)} \mathbb{E}_P [\tilde{\ell}(\xi)].$$

By Theorem 3.1, P_t^* is discrete with atoms $\{\hat{\xi}_i - \frac{q_{ik}^*}{\alpha_{ik}^*}\}$ and weights α_{ik}^*/N .

- 7: **(Policy Update):** Update θ_{t+1} by minimizing $\mathbb{E}_{P_t^*} [-\log \sigma(R_\theta(y_w) - R_\theta(y_l))]$ (or a logistic/contrastive variant), via standard gradient methods.
- 8: **end for**
- 9: **return** θ_T (final policy).

E. SSAPO algorithm and Analysis on Computational Complexity

E.1. The SSAPO algorithm

E.2. Computational Complexity of SSAPO

In this subsection, we analyze the computational costs incurred by each step of the Stackelberg Self-Annotated Preference Optimization (SSAPO) algorithm (Algorithm 1). We denote:

- N : the total number of preference pairs in the dataset \mathcal{D} at a given iteration,
- K : the number of linear pieces used in the concave piecewise approximation of $-\log \sigma(\xi)$,
- T : the total number of outer iterations for SSAPO.

We assume each *iteration* refers to Steps 1–5 of Algorithm 1.

Step 1 (Self-Annotation) The cost of self-annotation depends on the number of prompts and the policy's inference procedure. Let M_t denote the number of new prompts labeled at iteration t . Generating and ranking responses under π_{θ_t} typically dominates this step. If:

- G_t is the number of candidate responses generated per prompt,
- $C_{\text{inference}}$ is the average cost of a single forward pass (token generation) under π_{θ_t} ,

then the time complexity for Step 1 is approximately

$$\mathcal{O}(M_t \cdot G_t \cdot C_{\text{inference}}),$$

plus any overhead for storing new winner–loser pairs in \mathcal{D} . Since the number of newly added preferences grows over iterations, N itself typically increases from iteration to iteration.

Step 2 (Forming \hat{P}_N) Once \mathcal{D} is updated, we compute $\hat{\xi}_i = R_{\theta_t}(y_w^i) - R_{\theta_t}(y_l^i)$ for each pair. The cost here depends on:

- N , the current size of \mathcal{D} ,
- C_{reward} , the average cost to compute $R_{\theta_t}(y) = \beta \log \frac{\pi_{\theta_t}(y|x)}{\pi_{\text{ref}}(y|x)}$ for a given response y .

Because each preference pair requires evaluating R_{θ_t} on (y_w^i, y_l^i) , this step has complexity

$$\mathcal{O}(N \cdot C_{\text{reward}}).$$

In practical implementations, $R_{\theta_t}(y)$ often just reads off the log-probabilities from π_{θ_t} and π_{ref} at the final tokens, making C_{reward} similar to a single forward-pass cost per response.

Step 3 (Concave Piecewise Approximation) We construct K linear functions $\ell_k(\xi)$ such that $\tilde{\ell}(\xi) = \max_{1 \leq k \leq K} \ell_k(\xi) \leq -\log \sigma(\xi)$. In principle, one can precompute these K pieces over a small interval (e.g., $[0, 1]$) once and reuse them in every iteration. Hence, the complexity for updating or verifying the piecewise function at iteration t is typically:

$$\mathcal{O}(K),$$

assuming $\{\xi^{(k)}\}_{k=1}^K$ are fixed or can be quickly adapted based on the range of $\{\hat{\xi}_i\}$. This step is therefore relatively cheap compared to distributionally robust optimization.

Step 4 (Worst-Case Distribution) Step 4 solves the *distributionally robust optimization* (DRO) finite convex program

$$P_t^* = \arg \max_{P \in B_\epsilon(\hat{P}_N)} \mathbb{E}_P [\tilde{\ell}(\xi)].$$

The *naive* formulation (per (Mohajerin Esfahani & Kuhn, 2018)) becomes high-dimensional if N is large, because each sample point $\hat{\xi}_i$ and each piecewise component ℓ_k introduces auxiliary variables (such as α_{ik}, q_{ik}). Concretely, the number of decision variables can scale like $\mathcal{O}(N \cdot K)$, and the resulting linear or convex program might require $\mathcal{O}((NK)^\gamma)$ time in the worst case for some exponent $\gamma > 1$ (depending on the chosen solver and constraints).

However, several factors can reduce this cost:

- **Approximate Solvers.** In practice, specialized cutting-plane or primal-dual methods solve these DRO problems more efficiently than the worst-case theoretical bound.
- **Grouping Heuristics.** If one partitions the N samples into smaller groups (each of size $G < N$), the complexity per group is $\mathcal{O}((GK)^\gamma)$. Then one aggregates $M = \frac{N}{G}$ group-level solutions. This lowers the complexity significantly if $G \ll N$.

Hence, the worst-case step here is often $\mathcal{O}(N \cdot K)$ to $\mathcal{O}((NK)^\gamma)$, but can be much more tractable in practice with grouping or approximate methods. Regardless, Step 4 typically dominates the iteration complexity for large N .

Step 5 (Policy Update) Finally, we minimize

$$\mathbb{E}_{P_t^*} [-\log \sigma(R_\theta(y_w) - R_\theta(y_l))]$$

via standard gradient methods. Each gradient step requires sampling from (or reweighting by) P_t^* and evaluating $\sigma(\cdot)$, plus $R_\theta(y)$ for $y \in \{y_w, y_l\}$. If B is the mini-batch size for gradient descent, then each policy update epoch scales approximately as

$$\mathcal{O}(N \cdot C_{\text{reward}}),$$

assuming each of the N preference pairs in P_t^* can be sampled over multiple epochs. In many implementations, N can be large, so the training complexity depends heavily on how many gradient epochs or passes one uses at iteration t .

Overall Complexity per Iteration Putting the above pieces together, let us summarize the dominating terms:

1. *Self-Annotation (Step 1):* $\mathcal{O}(M_t \cdot G_t \cdot C_{\text{inference}})$,
2. *Forming \hat{P}_N (Step 2):* $\mathcal{O}(N \cdot C_{\text{reward}})$,
3. *Concave Piecewise Approx. (Step 3):* $\mathcal{O}(K)$,
4. *Worst-Case Distribution (Step 4):* $\mathcal{O}((NK)^\gamma)$ in the naive case, often reduced by grouping,
5. *Policy Update (Step 5):* $\mathcal{O}(N \cdot C_{\text{reward}} \cdot (\text{number of epochs}))$.

If we denote the cost of solving the DRO subproblem by $C_{\text{DRO}}(N, K)$ (which could itself be significantly reduced by grouping into subproblems of size G), then each iteration of SSAPO costs approximately:

$$\mathcal{O}\left(M_t \cdot G_t \cdot C_{\text{inference}} + N \cdot C_{\text{reward}} + C_{\text{DRO}}(N, K) + \dots\right).$$

In most scenarios, *either* the distributionally robust optimization (Step 4) *or* the gradient-based policy update (Step 5) will be the main bottleneck, depending on solver implementation and whether grouping is employed.

Total Complexity over T Iterations Over T total iterations, we multiply the above per-iteration cost by T . Additionally, note that N can increase each iteration if new self-annotated preferences are continuously appended to \mathcal{D} . Denoting N_t as the dataset size at iteration t , the total complexity from Steps 2–5 is roughly $\sum_{t=0}^{T-1} [\mathcal{O}(N_t \cdot C_{\text{reward}}) + C_{\text{DRO}}(N_t, K)]$, plus the self-annotation cost from Step 1. If N grows in a controlled manner (for example, linearly in t), the cumulative cost can be bounded accordingly.

Practical Guidelines.

- **Grouping for DRO.** To handle large N , we recommend partitioning the data into multiple groups $G \ll N$. The overall complexity then becomes $\mathcal{O}(M \cdot C_{\text{DRO}}(G, K))$, where $M = N/G$, which can be significantly faster in practice.
- **Caching Log-Probabilities.** The reward $R_{\theta_t}(y)$ can be computed from log-probabilities of π_{θ_t} and π_{ref} . Caching or reusing these values may reduce C_{reward} .
- **Adjusting K .** Increasing K refines the concave approximation but grows the size of the DRO problem. Hence, K is a hyperparameter balancing approximation quality and computational overhead.

Overall, the time complexity of SSAPO grows with N , K , and the iteration count T . By employing grouping and efficient solvers, We can typically achieve robustness benefits without incurring excessive computational cost.

F. More Details of Experimental Setups

F.1. Detailed Experimental Setups

We introduce more detailed experimental setups in Section 4 as follows.

Datasets. For preference learning, we employed the UltraFeedback dataset (Cui et al., 2023)⁴, aligning with prior research (Rosset et al., 2024; Kim et al., 2025). Specifically, we extracted a seed dataset comprising 2K samples (3.3% of the total 60K training samples), which included prompts, responses, and ground-truth preference labels. These ground-truth preference labels are referred to as gold labels in Table 1. The remaining training samples were then partitioned into three subsets of 8K, 20K, and 30K samples, retaining only the prompts. These subsets were utilized as the prompt sets for the 1st, 2nd, and 3rd iteration stages, respectively.

⁴[argilla/ultrafeedback-binarized-preferences-cleaned](https://argilla.ai/ultrafeedback-binarized-preferences-cleaned)

Models. Following previous work (Kim et al., 2025), we primarily conducted our experiments using the supervised fine-tuned Mistral-7B-0.1 model (Jiang et al., 2023a) as the initial model π_{init} . Specifically, we used the open-sourced model⁵ that follows the recipe of Zephyr (Tunstall et al., 2023) and is fine-tuned on the instructions of UltraChat (Ding et al., 2023). In Table 1, we also used LLaMA-3-8B⁶ to validate the compatibility of our method across different models. We used the generally fine-tuned models as there are no models that have been fine-tuned on the UltraChat dataset.

Evaluations. Following standard practices for aligning LLMs, we employed two primary evaluation benchmarks to assess model performance. First, we used **AlpacaEval 2.0** (Dubois et al., 2024a;b), a benchmark designed to approximate human preferences in instruction-following tasks. This evaluation involves 805 diverse instructions sourced from multiple datasets, where responses from the model under test are compared against those generated by GPT-4 (Achiam et al., 2023) to determine win rates. To address potential biases related to response length—a known factor influencing LLM preferences (Zheng et al., 2023; Wang et al., 2023), we report both the original win rate and a length-controlled (LC) win rate. The LC win rate is calculated using a regression model trained to neutralize the impact of response length, thereby focusing on the quality of the generated content (Dubois et al., 2024b).

Second, we employed **MT-Bench** (Zheng et al., 2023) to evaluate the model’s capabilities across a broader range of tasks. MT-Bench assesses a chatbot’s performance in areas such as math, coding, role-playing, and writing through multi-turn interactions. Responses are scored by GPT-4, providing a comprehensive measure of the model’s proficiency in key LLM functionalities. Together, these benchmarks offer a robust evaluation of how well the model aligns with human preferences and its effectiveness in real-world applications.

Implementation Details. In the initial alignment phase, we train the model using Direct Preference Optimization (DPO) on a seed dataset of 2K samples to obtain the base model π_0 . Following this, we conduct 3 iterative stages of data expansion. In the i -th iteration ($i = 1, 2, 3$), we generate preference data by independently sampling two responses for each prompt using a temperature of 0.7 and labeling them as chosen or rejected through $R(x, y)$, resulting in a preference dataset $\{\xi_i\}_{i=1}^N$ (N is the size of the i -th prompt set). Following SPA (Kim et al., 2025), we restricted the maximum token length for self-generated responses to 300 tokens. This limit corresponds to approximately 900 characters. To model the worst-case distribution program, we define a set of linear functions $\ell_k(x) = -\frac{K}{k}(x - \frac{k}{K}) - \log(\frac{k}{K})$ for $k = 1, \dots, K$ (the family of tangents of the loss function at the K -equipartition of $[0, 1]$). We solve the associated optimization program using the Sequential Least Squares Programming (SLSQP) method. The group size G is set to 100 unless otherwise specified for parallel computation of the convex program. Finally, we update the policy model by minimizing the reweighted loss to get π_i , ensuring improved alignment with the desired preferences.

Hyper-parameters for Different LLMs. For **Mistral-7B-0.1**, We set learning rate = 5×10^{-7} and DPO hyper-parameter $\beta = 0.1$ throughout the entire preference learning process. We conduct 3 epoch for the initial DPO training and 3 iteration for SSAPO game play (leader-follower updates).

For **LLaMA-3**, We set learning rate = 1×10^{-6} and DPO hyper-parameter $\beta = 0.05$ throughout the entire preference learning process. We conduct 1 epoch for the initial DPO training and 2 iteration for SSAPO game play (leader-follower updates).

F.2. Construction of Seed Data

Seed data (e.g. the initial labeled training data) has an impact on the performance of self-training algorithms. In our experiments, we explore two different methods of selecting seed data from the original training set, namely UltraFeedback dataset (Cui et al., 2023). Ground truth labels (e.g. the preferred and dispreferred response) of the selected seed data are retained, while the labels of the remaining data are discarded. As a result, our proposed method use only a small proportion of ground truth labels.

Random sampling. We select seed data from the entire training dataset randomly.

Farthest point sampling. Intuitively, the distribution of the seed data should “cover” as much part of the entire training dataset as possible, such that subsequent self-training iterations won’t suffer from distribution shift. With this motivation, we first leverage the SFT model to obtain an embedding vector for each prompt in the dataset, and then use farthest point

⁵[alignment-handbook/zephyr-7b-sft-full](https://github.com/alignment-handbook/zephyr-7b-sft-full)

⁶[meta-llama/Meta-Llama-3-8B-Instruct](https://huggingface.co/meta-llama/Meta-Llama-3-8B-Instruct)

sampling algorithm to select a subset of the embeddings (and corresponding preference pairs) as seed data. Specifically, we feed each prompt into the SFT model, and extract the hidden state of the last token of the last layer as the embedding. We use cosine similarity as the distance metric for embedding vectors.

In our implementation, we find that Mistral-7B model is not sensitive to either seed data sampling method. And LLama-8B model enjoy a slightly better performance with respect to the farther point sampling.

F.3. Infrastructure

For all experiments, we utilized 4 A800 GPUs. Under this computational resource, generating responses for 10K prompts takes approximately 15 minutes, and preference judging for generated responses takes about 30 minutes. Solving worst-case distribution with Eq. 17 takes about 40 minutes. Policy update takes about 1 hour per 10K training data.

G. Qualitative Examples

In this section, we present qualitative examples of the responses from the models trained under different methods: DPO (only train on initial seed data using DPO), SPA(Kim et al., 2025), and SSAPO (our proposed method). The results are presented below. These examples show that the model trained under SSAPO provides more detailed and precise responses to various questions.

Prompt:

The given text must be classified as offensive or not offensive.

You acted really crazy last night.

DPO response:

I do not have any information about the specific context or situation in which the statement you acted really crazy last night was made. Therefore, I am unable to determine whether it is classified as offensive or not. Please provide more context or details about the situation so that I can provide a more accurate response.

SPA response:

Based on the given text, it can be classified as "offensive" because it uses a colloquial and informal expression ("acted really crazy") to describe someone's behavior, which may convey a negative or derogatory connotation towards the person's actions. In formal or professional contexts, using such language may be considered inappropriate or unprofessional, and it could potentially offend the person involved or others who may be present. Using precise and objective language to describe behavior or actions is generally recommended in such situations to avoid any potential offense or misunderstanding. Therefore, using a more neutral or appropriate expression, such as "displayed unconventional behavior last night," may be a better option in this case.

SSAPO response:

Based on the given text "You acted really crazy last night," it is difficult to determine whether it is classified as offensive or not offensive. The text does not contain any explicit or direct insults, profanities, or derogatory language directed towards the person addressed. The phrase "acted really crazy" could be interpreted as a subjective assessment of the person's behavior or actions during the previous night, and may not necessarily be intended as an insult or criticism.

However, the tone or context in which the text is used could influence its perceived offensiveness. If the phrase "acted really crazy" is used sarcastically or with a condescending tone, it may be interpreted as an indirect insult or criticism aimed at the person's behavior or character. Alternatively, if the phrase is used casually or with a neutral tone, it may be interpreted as a straightforward observation or comment on the person's actions without any malicious intent.

In summary, the given text "You acted really crazy last night" may or may not be classified as offensive, depending on the tone, context, and intended meaning behind the phrase. Without additional information or context, it cannot be definitively

labeled as either offensive or not offensive.

Prompt:

Verify the correctness of the given statement.

”For all integers j and k, if j and k are odd, then jk is odd.”

DPO response:

The statement ”For all integers j and k, if j and k are odd, then jk is odd” is correct.

Proof:

Let j and k be any two odd integers.

Since j and k are both odd, there exist positive integers a and b such that:

$$j = 2a + 1 \text{ and } k = 2b + 1$$

where a and b are integers.

Multiplying j and k, we get:

$$\begin{aligned} jk &= (2a + 1)(2b + 1) \\ &= 2(2ab + a + b) + 1 \\ &= 2(2a*2b + a + b) + 1 \\ &= 2(2a*2b + 1) + (2*a + 2*b + 1) \end{aligned}$$

Since $2a$ and $2b$ are even integers, the product $2(2a*2b + 1)$ is an odd integer. Also, $(2*a + 2*b + 1)$ is an odd integer since it is of the form $2*c + 1$ where c is the sum of two even integers ($2a$ and $2b$). Therefore, jk is an odd integer.

Hence, for all integers j and k, if j and k are odd, then jk is odd.

Q.E.D.

SPA response:

The statement ”For all integers j and k, if j and k are odd, then jk is odd” is correct.

To prove this statement, we can use mathematical induction on the sum of the absolute values of j and k, denoted by $|j| + |k|$.

First, consider the base case where $|j| + |k| = 1$. In this case, either $j = 1$ and $k = 0$ or $j = 0$ and $k = 1$. In both cases, $jk = 1$, which is odd.

Next, assume the statement holds for all pairs of integers j and k such that $|j| + |k| = n$, where n is a positive integer. Let j and k be any two integers such that $|j| + |k| = n + 2$. Then, either $|j| = n + 1$ and $|k| = 1$ or vice versa. Without loss of generality, let $|j| = n + 1$ and $|k| = 1$. Then, $j = n + 1$ and $k = 1$ or $j = -(n + 1)$ and $k = -1$. In both cases, $jk = (n + 1) * 1 = n + 1$, which is odd by the induction hypothesis.

By mathematical induction, the statement holds for all integers j and k if j and k are odd, and jk is odd. Thus, the statement is correct.

SSAPO response:

The given statement ”For all integers j and k, if j and k are odd, then jk is odd” is correct.

To prove this statement, we need to show that for all integers j and k, if both j and k are odd, then their product jk is also odd.

Let j and k be two odd integers, i.e., $j = 2n + 1$ and $k = 2m + 1$, where n and m are any integers.

Then, their product jk can be written as:

$$jk = (2n + 1) * (2m + 1) = 4nm + 2n + 2m + 1 = 2(2nm + n + m) + 1$$

Since n, m are integers, the product $2nm + n + m$ is also an integer. Therefore, the above expression jk is equal to the sum of an even number ($2(2nm + n + m)$) and an odd number (1).

As the sum of two odd numbers is always even, the sum $2(2nm + n + m) + 1$ is an odd number.

Hence, the product $jk = (2n + 1) * (2m + 1) = 2(2nm + n + m) + 1$ is an odd integer, which proves the given statement.

Therefore, the given statement "For all integers j and k , if j and k are odd, then jk is odd" is correct.

Prompt:

Find the answer that best describes the underlined SAT word. Select the correct option and explain the meaning of the underlined word.

Despite the cacophony, the student tried to study.

- A. Loud sounds
- B. Difficult subject
- C. Late hour
- D. Low lighting

DPO response:

The correct option is A. Loud sounds. The word cacophony means "a loud and confusing mixture of sounds." In this sentence, it describes the noise level in the environment where the student is trying to study. Therefore, the underlined word cacophony refers to the loud sounds that are making it difficult for the student to concentrate.

SPA response:

- A) Loud sounds (cacophony)

Explanation:

The word "cacophony" refers to a loud and unpleasant combination of sounds, typically characterized by a discordant or confusing mixture of noise. In the context of the sentence, "despite the cacophony" suggests that the student is trying to study despite the overwhelming and distracting noise around them. The underlined word "cacophony" modifies the phrase "loud sounds" and provides a descriptive adjective.

Option B) Difficult subject, C) Late hour, and D) Low lighting are not relevant to the given context as they do not refer to loud or unpleasant sounds. Option A) "loud sounds" is a synonym for "cacophony" and accurately describes the situation mentioned in the sentence.

Therefore, the correct option for the underlined word is A) Loud sounds (cacophony).

SSAPO response:

Option A: "Despite the cacophony, the student tried to study"

The underlined word "cacophony" means a loud or chaotic combination of sounds. It describes a situation where there is an overwhelming or unpleasant mixture of noise or sounds.

Cacophony is derived from the Greek words "kakos" meaning "bad" or "ugly" and "phone" meaning "sound". It is commonly used to describe a variety of loud or unpleasant sounds, such as traffic noise, barking dogs, screaming children, or discordant music. In the given sentence, the student is trying to study despite the distracting and disruptive noise or sounds, which creates a cacophony. The word "despite" implies that the student is facing an obstacle or hindrance, which is the excessive noise or chaos, but they still persist in their efforts to concentrate and study.

Therefore, the meaning of the underlined word "cacophony" is a loud or chaotic combination of sounds, which creates an unpleasant or distracting environment for the student's studying. Option A is the correct answer. Option B refers to a difficult subject, Option C refers to a late hour, and Option D refers to low lighting, none of which are relevant to the given context.
